12 BS

VSC-TR-81-19

REGIONAL PHASE PROCESSORS

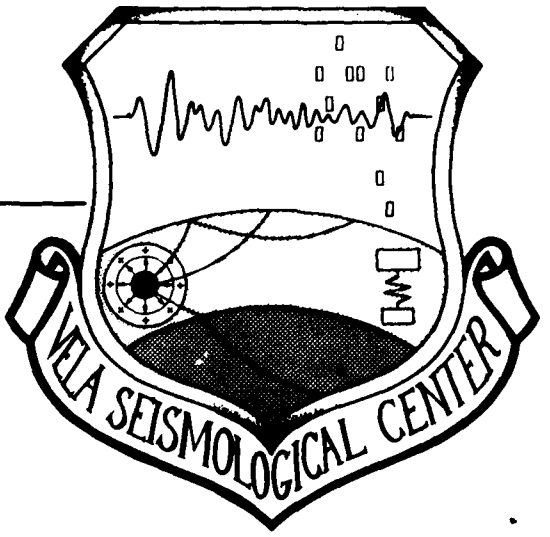

Eugene Smart & Helene Sproules
Seismic Data Analysis Center
Teledyne Geotech
314 Montgomery Street
Alexandria Virginia 22314

7 OCT 1981

APPROVED FOR PUBLIC RELEASE; DISTRIBUTION UNLIMITED.

Monitored By:
VELA Seismological Center
312 Montgomery Street
Alexandria, VA 22314

Sponsored by

The Defense Advanced Research Projects Agency (DARPA)

DARPA Order No. 2551

Unclassified

SECURITY CLASSIFICATION OF THIS PAGE (When Data Entered)

REPORT DOCUMENTATION PAGE

READ INSTRUCTIONS, BEFORE COMPLETING FORM

1. REPORT NUMBER: VSC-TR-81-19	2. GOVT ACCESSION NO.: AD-A105 470
3. RECIPIENT'S CATALOG NUMBER:	
4. TITLE (and Subtitle): REGIONAL PHASE PROCESSORS.	5. TYPE OF REPORT & PERIOD COVERED: Technical rept.,
6. PERFORMING ORG. REPORT NUMBER: SDAC-TR-81-1	
7. AUTHOR(s): Eugene Smart; Helene Sproules	8. CONTRACT OR GRANT NUMBER(s): F08606-79-C-0007; ARPA Order-2551
9. PERFORMING ORGANIZATION NAME AND ADDRESS: Teledyne Geotech, 314 Montgomery Street, Alexandria, Virginia 22314	10. PROGRAM ELEMENT, PROJECT, TASK AREA & WORK UNIT NUMBERS: VT/9709
11. CONTROLLING OFFICE NAME AND ADDRESS: Defense Advanced Research Projects Agency, 1400 Wilson Boulevard, Arlington, Virginia 22209	12. REPORT DATE: 3 March 1981
	13. NUMBER OF PAGES: 37
14. MONITORING AGENCY NAME & ADDRESS (if different from Controlling Office): VELA Seismological Center, 312 Montgomery Street, Alexandria, Virginia 22314	15. SECURITY CLASS. (of this report): Unclassified
	15a. DECLASSIFICATION/DOWNGRADING SCHEDULE: 7 Oct 81

16. DISTRIBUTION STATEMENT (of this Report): 39

APPROVED FOR PUBLIC RELEASE; DISTRIBUTION UNLIMITED.

17. DISTRIBUTION STATEMENT (of the abstract entered in Block 20, if different from Report)

18. SUPPLEMENTARY NOTES

19. KEY WORDS (Continue on reverse side if necessary and identify by block number)

Maximum-Likelihood
Three-Component Processing
Particle Motion
Phase Identification

20. ABSTRACT (Continue on reverse side if necessary and identify by block number)

The purpose of this study is to evaluate the principle of the technique known as the Smart processor, developed at the SDAC (Smart, 1977) and to determine the propagation direction of regional seismic phase by operating on a comprehensive data set.

The Smart single-station maximum-likelihood surface-wave processor and variants thereof, all relying on three-component particle-motion analysis, demonstrated in this study their utility for automatic signal azimuth determination.

DD FORM 1 JAN 73 1473 EDITION OF 1 NOV 65 IS OBSOLETE

Unclassified

SECURITY CLASSIFICATION OF THIS PAGE (When Data Entered)

408258

LB

In this study the Smart processor was found to be that which simply maximized the ratio of energy between components. Thus the P wave azimuth is determined by minimizing the transverse component, the L_g by maximizing the transverse and the emergence cycle by finding the best rectilinear motion fit to 3 components of data. For the entire test data set, the average azimuthal error was 6.7 degrees for the L_g signals, and 7.0 degrees for the P arrivals. Combining the estimated L_g azimuth with that of the P wave, simply by taking their mean, increased the accuracy. The average difference between the mean estimated azimuth and the true geodesic azimuth was 4.9 degrees (7.0 degrees rms). Moreover, the F-statistic computed by these processors serves to separate poor azimuthal estimates from the population: the azimuthal estimates (over 80% for this data set) which passed the arbitrary F threshold set for this study differed from the known geodesic azimuths by an average of 3.9 degrees (4.9 degrees rms). It is the author's experience that such accuracy is comparable to or better than that from a well-designed array of sensors.

Besides this, the results of the study suggest that particle-motion analysis can also be used to pick seismic phases automatically and that it can be made to yield automatic distance determinations simultaneously with the azimuth measurements. One complete source-location determination could thus be made for each station recording an event.

REGIONAL PHASE PROCESSORS

SEISMIC DATA ANALYSIS CENTER REPORT NO.: SDAC-TR-81-1

AFTAC Project Authorization No.:	VELA VT/9709
Project Title:	Seismic Data Analysis Center
ARPA Order No.:	2551
Name of Contractor:	TELEDYNE GEOTECH
Contract No.:	F08606-79-C-0007
Date of Contract:	October 1, 1979
Amount of Contract:	$1,493,393
Contract Expiration Date:	30 September 1980
Project Manager:	Robert R. Blandford (703) 836-3882

P. O. Box 334, Alexandria, Virginia 22313

APPROVED FOR PUBLIC RELEASE; DISTRIBUTION UNLIMITED.

ABSTRACT

The purpose of this study is to evaluate the principle of the technique known as the Smart processor, developed at the SDAC (Smart, 1977) and to determine the propagation direction of regional seismic phases by operating on a comprehensive data set.

The Smart single-station maximum-likelihood surface-wave processor and variants thereof, all relying on three-component particle-motion analysis, demonstrated in this study their utility for automatic signal azimuth determination.

In this study the Smart processor was found to be that which simply maximized the ratio of energy between components. Thus the P wave azimuth is determined by minimizing the transverse component, the L_g by maximizing the transverse, and the emergence cycle by finding the best rectilinear motion fit to 3 components of data. For the entire test data set, the average azimuthal error was 6.7 degrees for the L_g signals, and 7.0 degrees for the P arrivals. Combining the estimated L_g azimuth with that of the P wave, simply by taking their mean, increased the accuracy. The average difference between the mean estimated azimuth and the true geodesic azimuth was 4.9 degrees (7.0 degrees rms). Moreover, the F-statistic computed by these processors serves to separate poor azimuthal estimates from the population: the azimuthal estimates (over 80% for this data set) which passed the arbitrary F threshold set for this study differed from the known geodesic azimuths by an average of 3.9 degrees (4.9 degrees rms). It is the author's experience that such accuracy is comparable to or better than that from a well-designed array of sensors.

Besides this, the results of the study suggest that particle-motion analysis can also be used to pick seismic phases automatically and that it can be made to yield automatic distance determinations simultaneously with the azimuth measurements. One complete source-location determination could thus be made for each station recording an event.

TABLE OF CONTENTS

LIST OF FIGURES

LIST OF TABLES

INTRODUCTION

This study was prompted by the modest success of an experiment (Smart, 1977) in which a single-station, surface-wave, particle motion processor was applied to certain regional seismic surface-wave data. The signals, combined L_g-R_g waves from the underground nuclear explosions GNOME and SALMON, were recorded at several Long Range Seismic Measurement (LRSM) stations in 1961 and 1964 respectively. The processor, which fits a combined, fundamental-mode Rayleigh wave and Love wave to given 3-component seismic records, would seem ill-suited for application to short-period surface waves recorded at distances of no more than 30 degrees from the source. However, in spite of the evident mixture of higher modes in the records, fairly reasonable azimuths were estimated with the processor, although it could not be said to have detected the signals.

In this study the surface-wave processor is applied again to regional surface waves, and another processor, suitable for first-arrival P waves, is developed and applied to a test data set of seismic signals recorded at regional distances. The objective is to test the usefulness of such single-station particle-motion processor for detecting, identifying, locating, and analyzing seismic regional phases.

P-Wave Processing

Since P-wave particle motion is often quite irregular, departing widely from the simple motion that an homogeneous earth would produce, (see Figure 1), it is desirable that a P-wave processor not be restricted to fitting data to a model of straight-line, back-and-forth motion. Here we develop a process which merely searches out the orientation, azimuth and incidence angle in which the mean square excursion of the data is greatest, at least in the frequency band of interest, without explicitly modeling linear motion. However, in spite of our maneuver, this development is identical to fitting a straight-line motion model to the data, though we do not explicitly invoke the model in our development. This identity will be demonstrated after the development of the processor, which follows here.

It might be thought that this processor is similar to "remode" a non-linear processor discovered by Flinn in Archambeau et. al. (1965). The present processor, however, is linear and from this difference come several features which make it superior to remode.

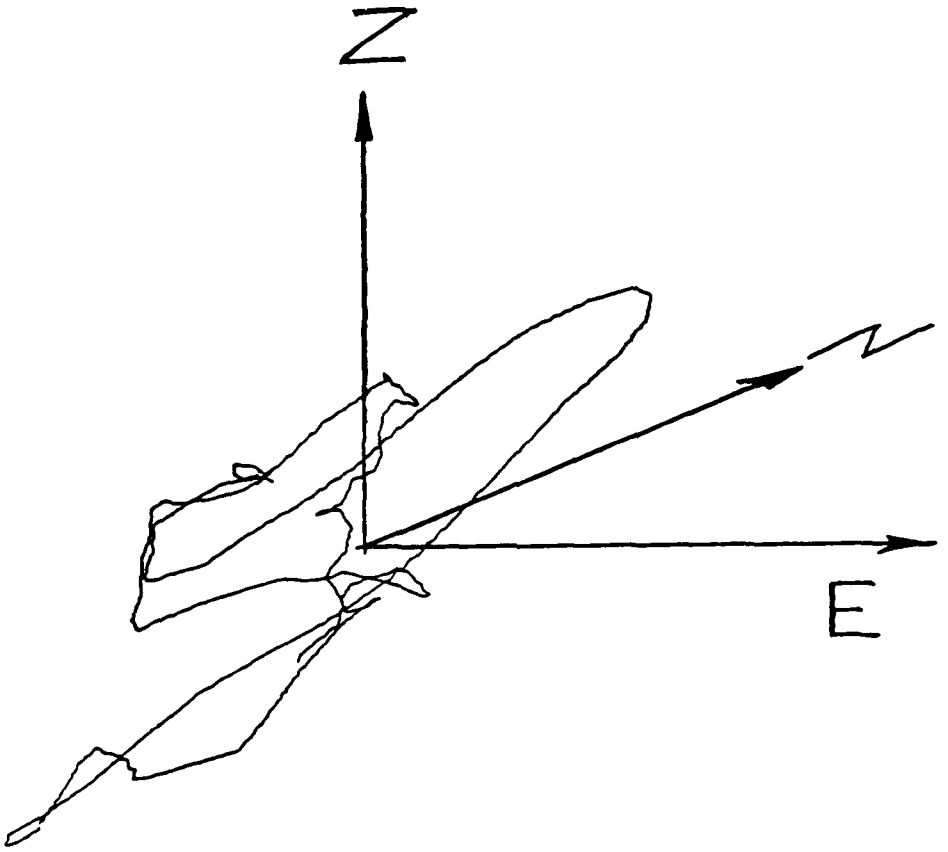

Figure 1. An example of P-wave particle motion, illustrating its irregularity.

Development of a P-Wave Processor

From Figure 2

$$r = z\cos\phi + y\sin\phi\cos\Theta + x\sin\phi\sin\Theta$$

or

$$r = \gamma z + \alpha\,\delta y + \beta\delta x$$

in which

$$\gamma = \cos\,\phi \qquad \delta = \sin\,\phi$$

and

$$\alpha = \cos\,\Theta \qquad \beta = \sin\,\Theta$$

The component of displacement in the r direction at the i^{th} sampling instant is, then

$$r_i = \gamma z_i + \alpha\delta y_i + \beta\delta x_i$$

The sum of the squared excursion along the r direction is

$$\nu \equiv \sum_{i=1}^{N} r_i^2$$

over the time interval i=1,...,N.

To move into the frequency domain observe that

$$\nu \equiv \sum_{i=1}^{N} r^2 = \sum_{j=0}^{\frac{N}{2}} |\Psi_j|^2$$

in which the Ψ_j are complex coefficients of the $\frac{N}{2} + 1$ terms of the discrete Fourier transform.

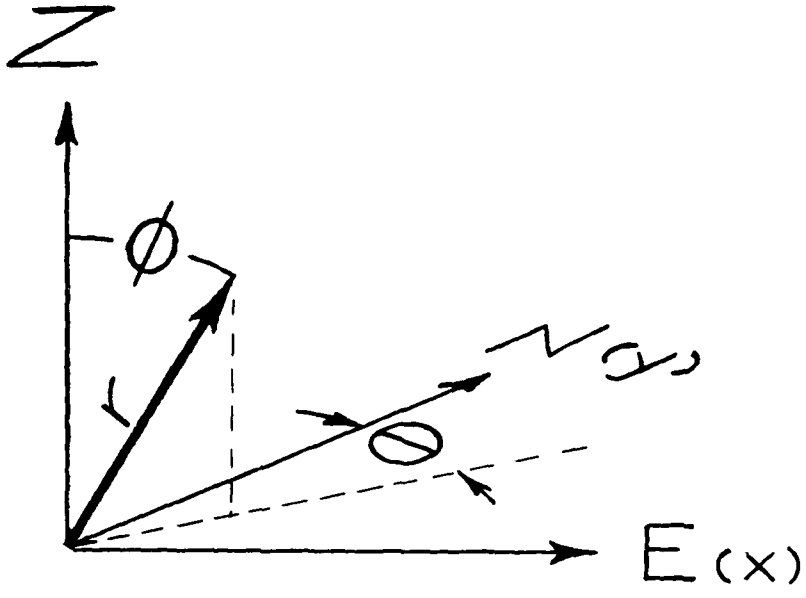

Figure 2. Reference figure for P-processor development (see text).

Let

$$\Psi_j \equiv R_j + iR'_j$$

in which

$$R_j = \text{real } [\Psi_j]$$

and $$R'_j = \text{imaginary } [\Psi_j]$$

$$R_j = \gamma Z_j + \alpha\delta Y'_j + \beta\delta X_j$$

and $$R'_j = \gamma Z'_j + \alpha\delta Y'_j + \beta\delta X'_j$$

So

$$|\Psi_j|^2 = R_j^2 + R_j'^2$$

and

$$\nu \equiv \sum_{i=1}^{N} r_i^2 = \sum_{j=0}^{\frac{N}{2}} [\gamma Z_j + \alpha\delta Y_j + \beta\delta X_j]^2 + [\gamma Z'_j + \alpha\beta Y'_j + \beta\delta X'_j]$$

Should we choose to do so, we are able to compute the mean squared excursion in a limited band

$$\nu_{m,n} = \sum_{j=m}^{n} R_j^2 + R_j'^2$$

in which m and n are arbitrary integers such that

$$0 \leq m < n$$

$$m < n \leq \frac{N}{2}$$

Then

$$\nu_{m,n} = \beta^2\delta^2 A + \alpha^2\delta^2 B + \gamma^2 C + \alpha\beta\delta^2 D + \beta\gamma\delta F + \alpha\gamma\delta G$$

where

$$A = \sum_{j=m}^{n} X_j^2 + X_j'^2$$

$$B = \sum_{j=m}^{n} Y_j^2 + Y_j'^2$$

$$C = \sum_{j=m}^{n} Z_j^2 + Z_j'^2$$

$$D = 2\sum_{j=m}^{n} X_j Y_j + X_j' Y_j'$$

$$F = 2\sum_{j=m}^{n} X_j Z_j + X_j' Z_j'$$

$$G = 2\sum_{j=m}^{n} Y_j Z_j + Y_j' Z_j'$$

Dropping the subscription on ν

$$\nu = \gamma^2 b_1 + \delta\gamma b_2 + \delta^2 b_3$$

in which

$$b_1 = C$$

$$b_2 = \beta F + \alpha G$$

$$b_3 = \alpha^2 B + \beta^2 A + \alpha\beta D$$

Then

$$2\nu = b_1 + b_3 + \mu(b_1 - b_3) + \zeta b_2$$

in which

$$\zeta = \sin 2\phi \text{ and } \mu = \cos 2\phi$$

Maximizing ν with respect to ϕ, the incidence angle, for arbitrary azimuth Θ,

$$\frac{\partial \nu}{\partial \phi} = -\zeta(b_1 - b_3) + \mu b_2 = 0$$

$$\zeta = b_2/\text{den}$$

and

$$\mu = (b_1 - b_3)/\text{den}$$

in which

$$\text{den} = \sqrt{(b_1 - b_3)^2 + b_2^2}$$

Maximized with respect to ϕ, then

$$2\nu = b_1 + b_3 + [(b_1 - b_3)^2 + b_2^2]^{1/2}$$

Now maximizing ν with respect to azimuth, Θ,

$$\frac{2d\nu}{d\Theta} = b_5 + \frac{1}{2}[(b_1 - b_3)^2 + b_2^2]^{-1/2}[-2(b_1 - b_3)b_5 + 2b_2b_4] = 0$$

in which

$$b_4 = b_2' = \alpha F - \beta G$$

and

$$b_5 = b_3' = 2\alpha\beta(A - B) + (\alpha^2 - \beta^2)D$$

Then

$$b_5[(b_1 - b_3)^2 + b_2^2]^{1/2} = (b_1 - b_3)b_5 - b_2b_4$$

$$b_5^2(b_1 - b_3)^2 + b_5^2b_2^2 = (b_1 - b_3)^2b_5 + b_2^2b_4^2 - 2b_2b_4b_5\ (b_1 - b_3)$$

$$b_2(b_4^2 - b_5^2) = 2b_4b_5(b_1 - b_3)$$

This can be written in the form

$$\alpha^3 w + \alpha^2\beta x + \alpha\beta^2 y + \beta^3 z = 0$$

where

$$w = (D^2 - F^2)\ G - 2(B - C)DF$$

$$x = 4(A - B)(C - B)F - F[(F^2-G^2) + (D^2-G^2)] + [(A-B) + (A-C)]DG$$

$$y = 4(A-B)(A-C)G + G[(F^2-G^2) - (D^2-F^2)] - 2[(A-B) - (B-C)]DF$$

$$z = (D^2 - G^2)F - 2(A - C)DG$$

To eliminate β from the equation, note that

$$\alpha^3(w - y) + \alpha y = - \beta[\alpha^2(x - z) + z]$$

and square

$$\alpha^6(w - y)^2 + 2\alpha^4(w - y)y + \alpha^2 y^2 = \beta^2[\alpha^2(x - z) + z]^2$$

$$= \alpha^4(x - z)^2 + 2\alpha^2(x - z)z + z^2 - \alpha^6(x - z)^2$$

$$- 2\alpha^4(x - z)z - \alpha^2 z^2$$

This can be written in the form of a cubic equation in α^2:

$$(\alpha^2)^3 P + (\alpha^2)^2 Q + \alpha^2 R + S = 0$$

where now

$$P = (w - y)^2 + (x - z)^2$$

$$Q = 2(w - y)y + 2(x - z)z - (x - z)^2$$

$$R = y^2 - 2(x - z)z + z^2$$

$$S = -z^2$$

The solution we seek is restrained by these considerations:

1) $0 \leq \alpha^2 \leq 1$ on the real numbers

2) $-1 \leq \mu \leq 1$

and

$$0 \leq \zeta \leq 1$$

since

$$0 \leq \phi < \frac{\pi}{2}$$

from the constraint that the particle motion in the positive sense must be up and away from the source of the arriving P-wave.

The cubic equation can, of course, be solved analytically. Thus ν is optimized without a computer search, which ensures processing speed.

To show that this development is identical to modeling a straight-line, back-and-forth motion, consider such motion along azimuth θ and incident angle ϕ, having waveform r where r_i is the i^{th} sample in the time series representation of the model. The components of r in the 3 coordinate directions are

$$\beta\delta r, \ \alpha\delta r, \text{ and } \gamma r$$

for the x, y, and z axes respectively.

The error, ε, or the difference between the data and this model is

$$\varepsilon = \Sigma \ (z_i - \gamma r_i)^2 + (y_i - \alpha\delta r_i)^2 + (x_i - \beta\delta r_i)^2$$

where i extends over the time window of interest.

$$\varepsilon = \Sigma \ x_i^2 + y_i^2 + z_i^2 - 2\Sigma r_i \ (\gamma z_i + \alpha\delta y_i + \beta\delta x_i) + \Sigma r_i^2$$

To estimate the waveforms at the arbitrary azimuth, θ, and incident angle, ϕ, take the partial derivative of ε with respect to r_n, the n^{th} sample in the time series representation of the model.

$$\frac{\partial \varepsilon}{\partial r_n} = 2(\gamma z_n + \alpha\delta y_n + \beta\delta x_n) + 2r_n$$

Setting this to zero

$$r_n = \gamma z_n + \alpha\delta y_n + \beta\delta x_n$$

Substituting the r_n back into ε,

$$\varepsilon = \Sigma x_i^2 + y_i^2 + z_i^2 - 2\Sigma r_i^2 + \Sigma r_i^2$$

$$= \Sigma x_i^2 + y_i^2 + z_i^2 - \Sigma r_i^2$$

To optimize r with respect to Θ and ϕ we must minimize ε. Thus we must maximize

$$\Sigma r_i^2$$

But

$$\Sigma r_i^2 = \Sigma\ (\gamma z + \alpha\delta y + \beta\delta x)^2 = \nu$$

where ν is the same function we optimized in our earlier development.

Thus our maneuver to avoid explicitly invoking the straight-line back-and-forth P-wave model gains us nothing. The process of finding the azimuth and angle from the vertical at which the mean square excursion is maximized is identical to the process of estimating the azimuth and incident angle of a P-wave model of straight-line, back-and-forth motion.

A Surface-Wave Processor

The surface-wave processor described in the Teledyne Geotech report SDAC-TR-77-14 has been extended in this study; the ellipticity ratio is no longer a required input parameter but is estimated simultaneously with the azimuth and spectra. This feature has proved necessary since, in practice, we have not known the ellipticity ratios for the stations and frequencies (and azimuths) of the data we have processed and have had to guess them.

The development of the single mode surface-wave processor with unrestrained ellipticity follows, see Figure 3. (We shall see that a simple processor which uses only horizontal components and maximizes the transverse to residual energy ratio gives better results.)

We may represent the anticipated fundamental mode surface-wave by its three-component particle motion:

r_n	is the complex Fourier coefficient, at the n^{th} frequency, of the vertical component of Rayleigh wave displacement
$i\varepsilon_n r_n$	is the corresponding coefficient of the radial component, which leads the vertical by 90 degrees of phase angle and differs from it in amplitude by a factor ε_n (the ellipticity ratio)
ℓ_n	is the coefficient of the Love wave displacement, transverse to the Rayleigh displacement and unrelated to it in both phase and amplitude.

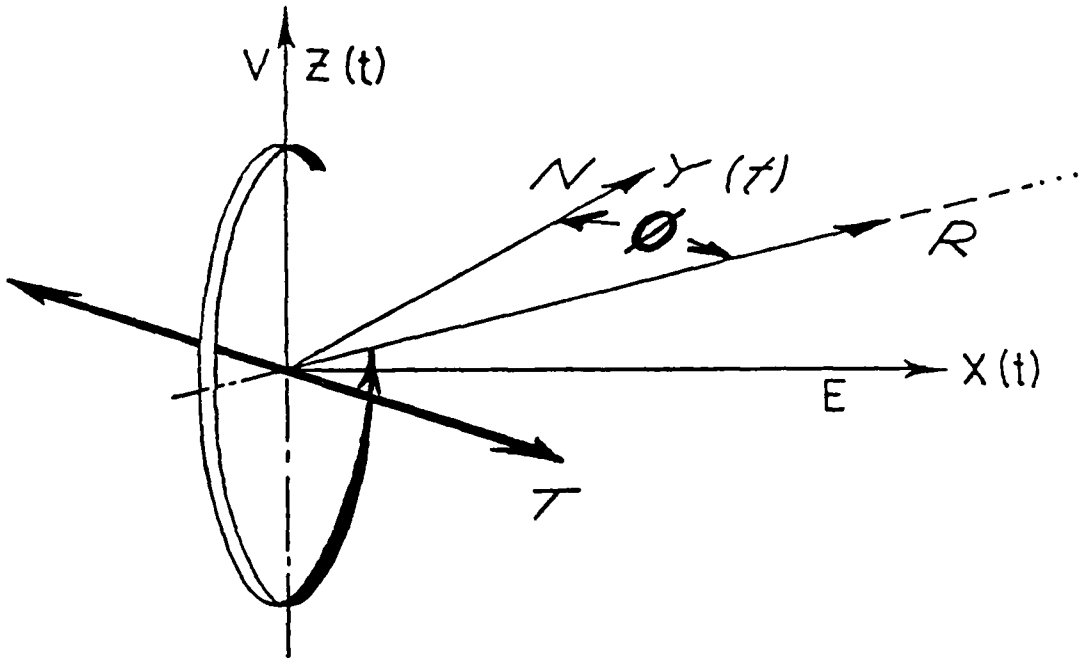

Figure 3. Illustration of fundamental mode Rayleigh-wave, Love-wave particle motion.

If the azimuth along which this signal model is propagating is ϕ, then the three-components we expect to record are

vertical: $\mathcal{r}_n$

north: $i\varepsilon_n \mathcal{r}_n \cos\phi - \mathcal{l}_n \sin\phi$

east: $i\varepsilon_n \mathcal{r}_n \sin\phi + \mathcal{l}_n \cos\phi$

If we let

$$\alpha \equiv \cos\phi \qquad\qquad \beta \equiv \sin\phi$$

then the sum of the squares of the difference between the data and the signal model may be written

$$E(\mathcal{r}_m, \mathcal{l}_m, \phi = \sum_n |z_n - \mathcal{r}_n|^2 + |y_n - (i\varepsilon_n \mathcal{r}_n \alpha - \mathcal{l}_n \beta)|^2 + |x_n - (i\varepsilon_n \mathcal{r}_n \beta + \mathcal{l}_n \alpha)|^2$$

The F-statistic for the model is given by

$$F(\mathcal{r}_m, \mathcal{l}_m, \phi) = \frac{\frac{1}{2} \Sigma (1 + \varepsilon_n^2)|\mathcal{r}_n|^2 + |\mathcal{l}_n|^2}{E(\mathcal{r}_m, \mathcal{l}_m, \phi)}$$

We may minimize E with respect to $\mathcal{r}_n$ and $\mathcal{l}_n$, the model spectra, in the usual fashion by taking the partial derivatives of E with respect to each of the real and imaginary parts of each of the spectral coefficients. Setting each derivative equal to zero we get

$$\mathcal{r}_n = (1 + \varepsilon_n^2)^{-1} \quad [z_n - i\varepsilon_n(\alpha y_n + \beta x_n)]$$

$$\mathcal{l}_n = \alpha x - \beta y_n$$

Substituting these results into E, the sum of the squares of the difference between the signal model and the data, we get

$$E(\phi) = \sum_n |i\varepsilon_n z_n - (\alpha y_n + \beta x_n)|^2 \ (1 + \varepsilon_n^2)^{-1}$$

If we assume now that ε_n is constant over the range of the summation, that is,

$$\varepsilon_n = \varepsilon, \text{ a constant with respect to } n$$

we may express E as

$$(1 + \varepsilon^2)E = \varepsilon^2 h + \alpha^2 g + \beta^2 d - 2\alpha\beta c - 2\varepsilon(\alpha a + \beta b)$$

in which

$$a \equiv \frac{i}{2} \sum_n (y_n^* z_n - y_n z_n^*)$$

$$b \equiv \frac{i}{2} \sum_n (x_n^* z_n - x_n z_n^*)$$

$$c \equiv -\frac{1}{2} \sum_n (y_n^* x_n + x_n^* y_n)$$

$$d \equiv \sum_n |x_n|^2$$

$$g \equiv \sum_n |y_n|^2$$

$$h \equiv \sum_n |z_n|^2$$

We now take the partial derivatives of E in this form, first with respect to ε, and then with respect to ϕ, and set each result to zero. Taking the partial derivative of E with respect to ε and setting it to zero yields

$$\varepsilon E = \varepsilon h - (\alpha a + \beta b)$$

Substituting this expression back into the previous equation, we eliminate E with the result that

$$A \varepsilon^2 + B\varepsilon - A = 0$$

in which

$$A = \alpha a + \beta b$$

$$B = h - (\alpha^2 g - 2\alpha\beta c + \beta^2 d)$$

Now, taking the partial derivative of E with respect to ϕ and setting it to zero yields

$$\varepsilon U = -V$$

in which

$$U = \alpha b - \beta a$$

$$V = \alpha\beta(g - d) + (\alpha^2 - \beta^2)c$$

Substituting this expression into

$$A\epsilon^2 + B\epsilon - A = 0$$

yields

$$V(AV - BU) - AU^2 = 0$$

Finally, substituting for A, B, U, and V, we have that

$$\alpha^3 W + \alpha\beta^2 X + \alpha\beta^2 Y + \beta^3 Z = 0$$

in which

$$W = a(c^2 - b^2) + (g - h)bc$$

$$X = ac(g + h - 2d) + b(g - h)(g - d) - b(b^2 + c^2 - 2a^2)$$

$$Y = bc(d + h - 2g) + a(d - h)(d - g) - a(a^2 + c^2 - 2b^2)$$

$$Z = b(c^2 - a^2) + (d - h)ac$$

This may be written as

$$Z \tan^3\phi + Y \tan^2\phi + X \tan\phi + W = 0$$

which is a cubic equation in $\tan\phi$. The cubic equation is, of course, solved analytically without computer search. This completes the development.

As noted above, the purpose of this study was to develop a regional event processor based upon the fundamental-mode surface-wave technique developed by Smart (1977). The study was successful and, among other things, it has enabled us to explain the past success of the technique as an azimuth estimator when applied to L_g phases.

Test Data Set

Thirty-one events recorded at RKON, well distributed azimuthally about the station and covering the spectrum of signal-to-noise ratios, were selected as a test data set for this study (Figure 4 and Table I). Signal and noise spectra have been computed for all the L_g phases. Figure 5 shows the spectra of four events, the two highest frequency and the two lowest frequency spectral maxima in the data set. (In general, the low-frequency signals were those which traversed complex mountainous regions on their way to RKON, e.g., events from California, Oregon, Washington, and British Columbia.)

Figure 5 also shows composite noise spectra by seasons. Contrary to expectations, the noise spectra were found not to vary significantly over the seasons. As can be seen in the figure, the noise peaks below 0.4 Hz, whereas all signal spectra peak at or above that frequency. This observation determined the lower edge of the frequency window chosen for L_g processing.

The Analysis

For the analysis of L_g waves the modified version of the Smart processor, which estimates particle motion ellipticity as well as azimuth and waveform, was used. Previously, ellipticity has been an input parameter. The frequency band examined was 0.5 and 3.0 Hz. The L_g windows, 51.2 seconds long, were hand picked by an analyst. Good back azimuths were obtained in general: the average of the absolute errors was 6.7 degrees (11.1 degrees rms). Some of the low-frequency events yielded the least accurate estimates.

A variety of parameters estimated by the L_g process was monitored during the experiment in a search for a suitable detection index, i.e., one which separates signals from noise. The parameters investigated were: the F-statistic, the mean recurrence period, and the derivative $\partial^2/E\partial\phi^2$,

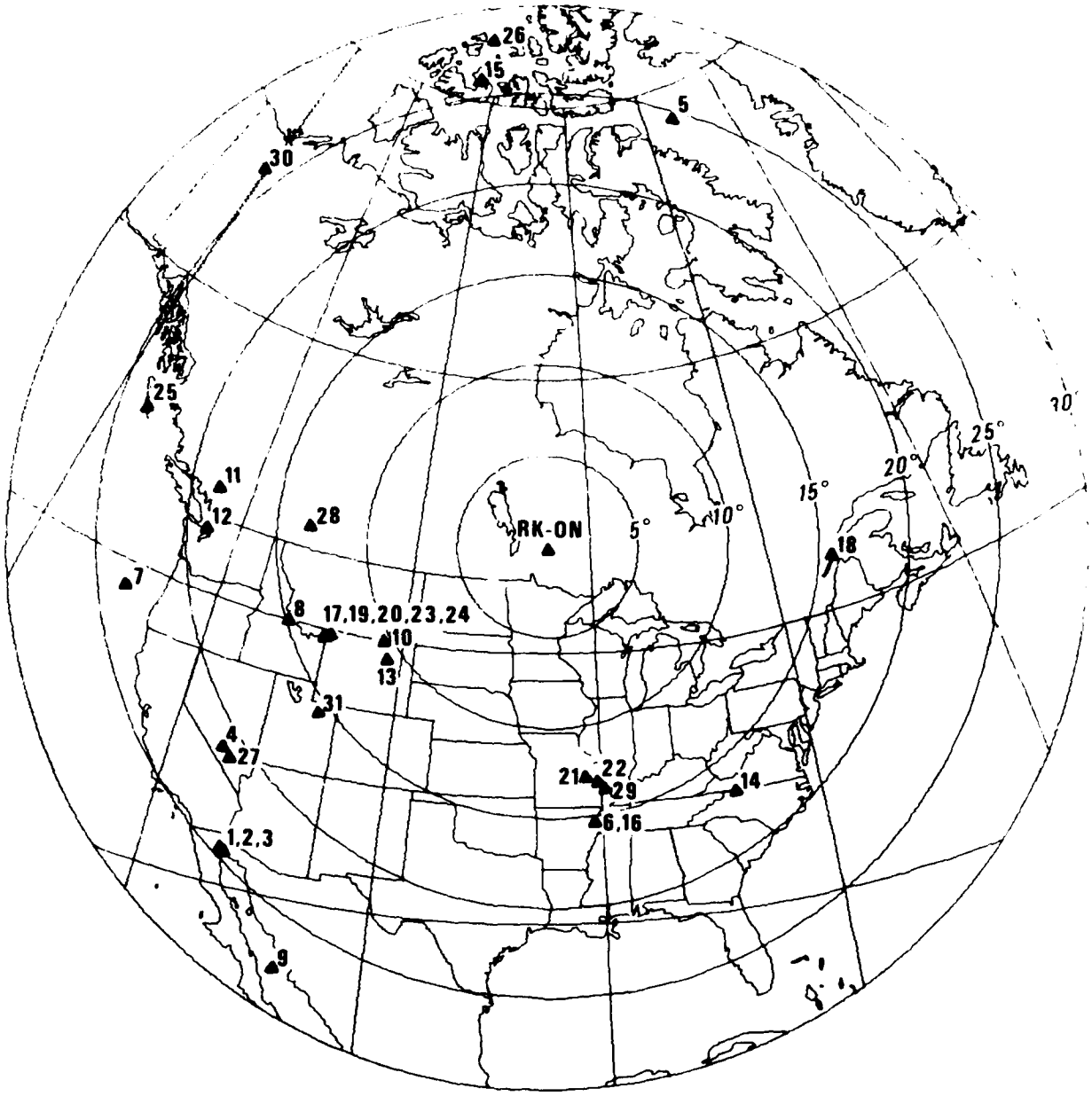

Figure 4. Epicenters of 31 regional seismic events recorded at Red Lake, Ontario (RKON). These 3-component records form the test data set for this report (see Table I).

TABLE I

REGIONAL EVENTS AT RKON

#	Date	Origin Time	Coordinates		Geographic Region	m_b	Δ°	φ°
1	11 Mar 78	23:57:45.3	31.9N	114.7W	Gulf of California	4.7	24.5	227
2	12 Mar 78	00:30:17.4	32.0N	115.0W	Southern California	4.1	24.5	227
3	12 Mar 78	18:42:24.1	32.0N	114.9W	W. Arizona-Mexico border	4.7	24.5	227
4	09 Mar 76	14:00:00.1	37.310N	116.364W	S. Nevada*	6.0	21.0	238
5	20 Mar 76	00:47:27.3	73.194N	68.899W	Baffin Bay	4.5	24.6	16
6	25 Mar 76	00:41:20.5	35.59N	90.48W	Arkansas	4.9	15.4	170
7	22 Apr 76	04:21:39.1	43.636N	127.005W	Off Coast of Oregon	4.2	23.5	265
8	26 Jul 76	10:45:28.2	49.022N	114.179W	Eastern Idaho	4.3	14.9	254
9	31 Jul 76	22:32:10.5	26.242N	110.338W	Gulf of California	4.8	27.7	213
10	10 Aug 76	13:54:57.2	45.029N	106.569W	Montana	3.4	10.4	241
11	12 Aug 76	06:28:59.0	50.62N	123.01W	British Columbia	3.8	18.4	280
12	02 Sep 76	13:16:11.0	48.205N	122.761W	Washington	4.3	18.9	273
13	03 Sep 76	04:18:16.2	44.041N	106.154W	Wyoming	4.8	10.8	235
14	13 Sep 76	18:54:37.1	36.604N	80.810W	North Carolina	3.3	16.9	142
15	16 Sep 76	10:14:39.0	76.136N	108.384W	Qu. Elizabeth Isls	4.6	25.9	352
16	25 Sep 76	14:06:56.6	35.61N	90.45W	Arkansas	3.6	15.4	170
17	19 Oct 76	07:24:34.0	44.795N	110.697W	Yellowstone Park, Wyo.	5.3	12.9	248
18	23 Oct 76	20:58:18.1	47.82N	69.79W	Gaspe Peninsula	3.8	15.8	91
19	27 Nov 76	00:24:46.1	44.639N	111.142W	Hebgen Lake	3.3	13.2	248
20	08 Dec 76	14:40:59.4	44.760N	110.793W	Yellowstone Park, Wyo.	5.5	13.0	248
21	11 Dec 76	07:05:00.9	38.12N	91.07W	Missouri	4.2	12.8	170
22	13 Dec 76	08:35:54.6	37.798N	90.236W	Eastern Missouri	3.5	13.3	168
23	19 Dec 76	17:10:15.7	44.772N	110.800W	Yellowstone Park, Wyo.	4.9	13.0	248
24	20 Dec 78	01:34:16.0	44.842N	110.827W	Yellowstone Park, Wyo.	4.4	12.9	249
25	13 Jan 78	08:25:34.5	52.8N	132.0W	Queen Charlotte Isl.	4.4	23.5	289
26	05 Feb 78	16:07:09.9	78.4N	107.8W	Queen Elizabeth Isls.	4.9	28.0	354
27	23 Feb 78	16:59:59.3	36.9N	45.9W	California-Nevada border	5.6	21.1	237
28	04 Mar 78	19:13:33.5	50.3N	114.4W	Alberta Province, Canada	3.5	13.1	275
29	03 Jan 77	22:56:48.6	37.55N	89.79W	Cape Girardeau, Mo., region	5.0	13.6	166
30	27 Jan 77	00:51:05.0	66.790N	135.433W	N. Yukon Territ., Canada	4.7	26.1	323
31	30 Sep 77	10:19:21.0	40.518N	110.436W	Utah	5.0	15.5	234

* explosion

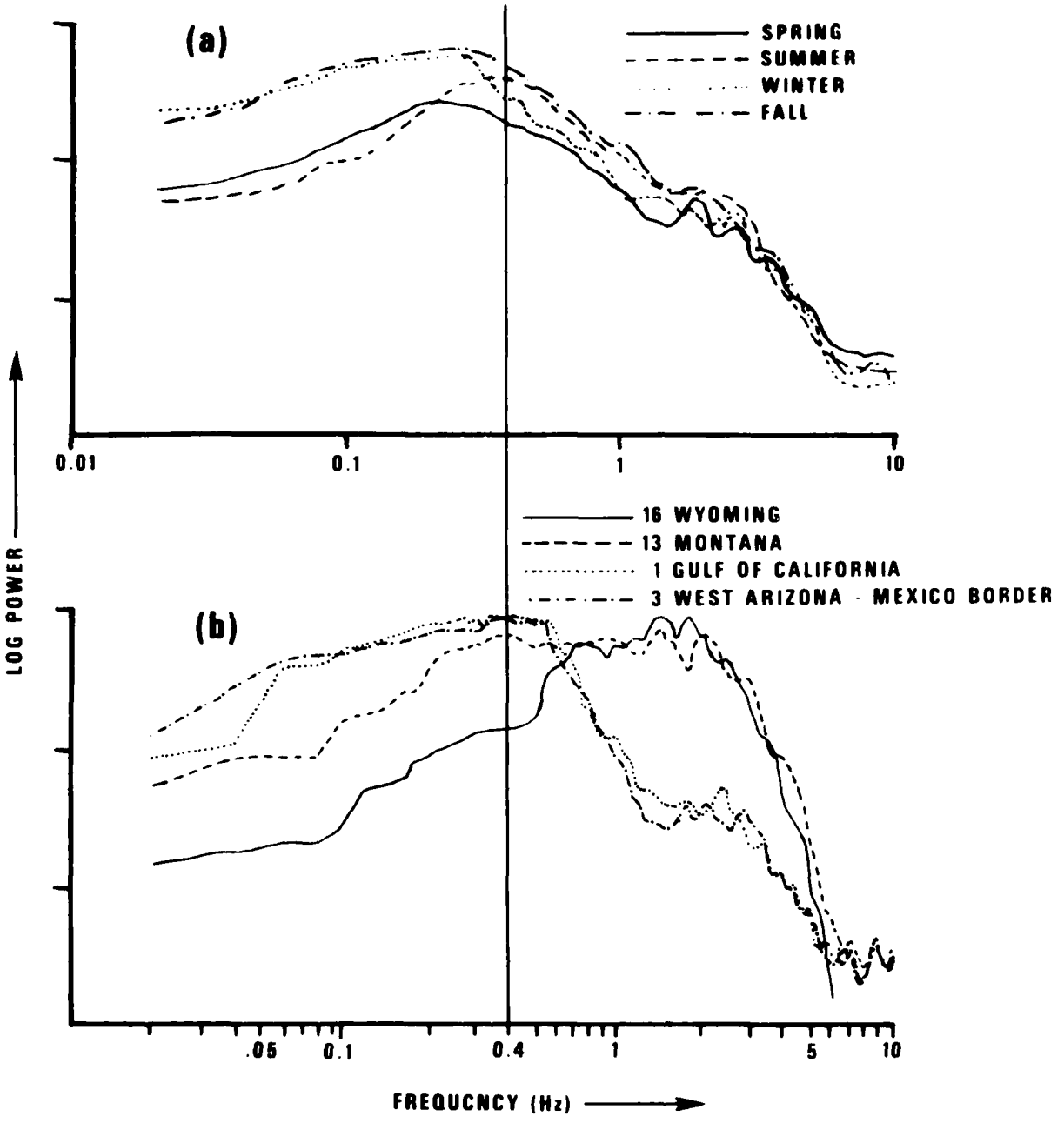

Figure 5. (a) Composite noise spectra for RKON, for four seasons.
(b) Peak-normalized spectra of the lowest- and highest-frequency event nos. 1, 3, 13 and 16 (see Table I).

where E = error and ϕ = back azimuth (see Smart, 1977). The rms excursions for the model in the vertical, radial, and transverse directions, denoted by Z, R, and T, were also examined.

The derivative did not follow a discernible pattern. The F-statistic and mean recurrence period were consistently low for both noise and signal and did not separate them (see Figure 6 for F-statistic histogram). The ratio T/R proved a somewhat useful discriminator, but its separation of the populations was not complete enough to qualify it as a detector (Figure 7). It was observed that T/R < 2.0, when it occurred, accompanied poor azimuthal estimates, i.e., error > 10 degrees, and that the smaller T/R, the larger the azimuthal error.

These observations suggested that, by itself, the figure traced by the particle motion in the horizontal plane might serve to indicate surface-wave azimuth. An algorithm was coded to find in each time window that orientation in the horizontal plane where the rms excursion, in the frequency band of interest, was minimized. The azimuth of the orientation was, on the average, about as good an estimate of surface wave origin as the back azimuth from the original coherent processor. Moreover, it was more stable. In low signal-to-noise records, where T/R fell below 2.0, the estimated azimuth was more accurate than that of the coherent processor. All this appears to explain why the Smart processor has been successful for estimating L_g azimuths, but unsuccessful for detecting L_g arrivals. The azimuth estimations have been controlled by the dominant transverse Love component, but the F-statistics have been kept low by the incoherence between the vertical and radial components. This incoherence results from the mixing of fundamental Rayleigh modes with higher ones.

The results suggested another use for this same simple algorithm which monitors the elongation of the figure described by particle motion, that is, to flag the arrival of P-waves and indicate their azimuths. 6.4 second time windows--an order of magnitude smaller than those for the L_g waves--were used to search in the vicinity of the expected P arrivals. The principal axis of the elongated figure was taken to indicate back azimuth, and the amount of elongation, that is, the ratio of the principal long axis to the short axis, was taken as the index of signal presence. Taking that ratio at 2.4 as the detection threshold, in the band 0.9 to 6.0 Hz,

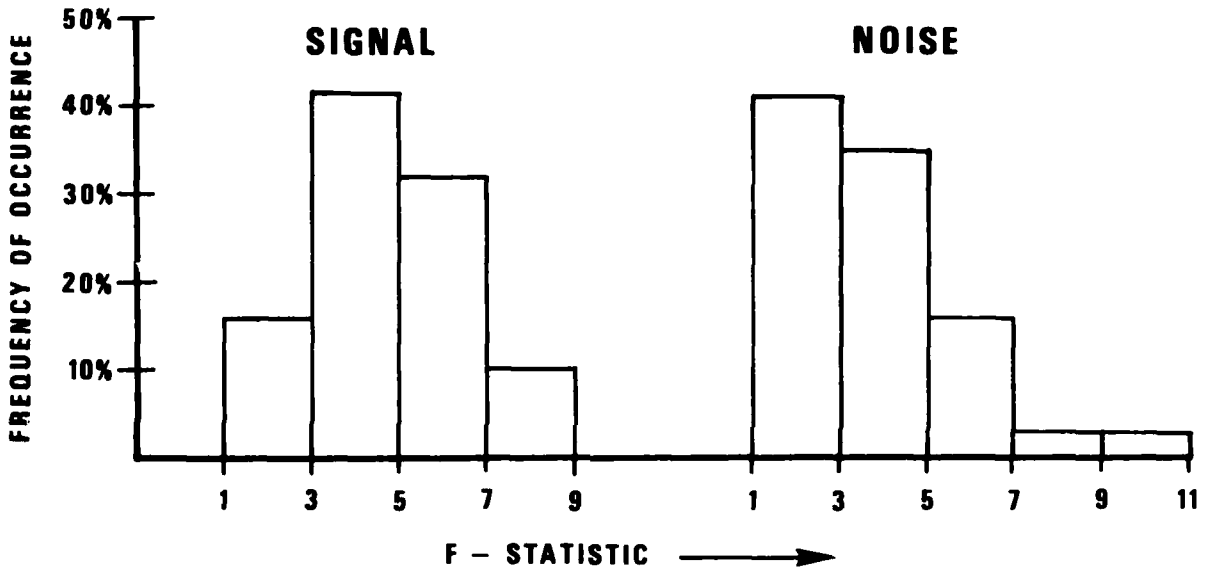

Figure 6. F-statistics for the noise and for the surface waves of the present test data set (see Table I) for the frequency band of 0.5 to 3.0 Hz show negligible separation of populations.

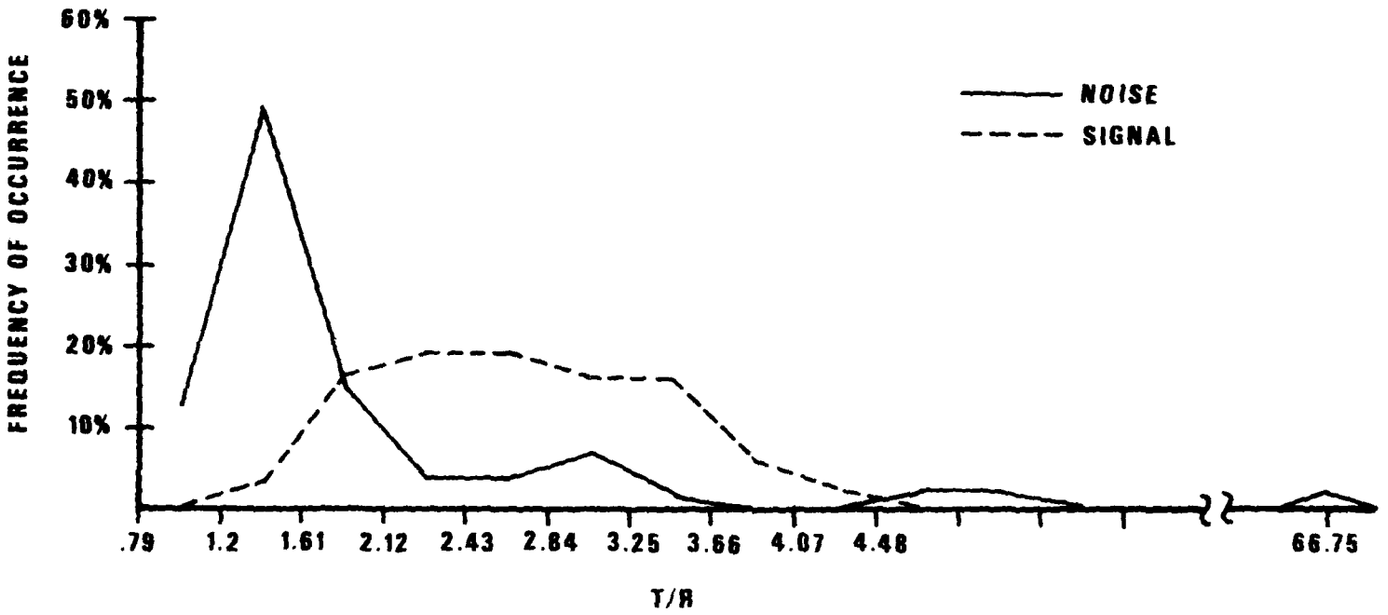

Figure 7. Separation of noise and surface-wave signal by T/R, the ratio of the estimated transverse excursion to that of the radial.

80% of the signals were detected with a high false alarm rate of 28 per hour. The average azimuthal error was 6.0 degrees, and, in the case of the low-frequency, low signal-to-noise events, these P azimuthal estimates were more accurate than those from the L_g waves. Thus, in spite of the high L_g/P amplitude ratios, the P wave appeared as useful for signal detection and for azimuth estimation as L_g, within the restraints of the present investigation.

However, this technique made use of only two components of the data, and in the next set of tests the three-component P-wave process, developed above, proved more useful. Since it estimates the emergence angle of the wave and thus takes account of the motion up and away from the source, P-wave particle motion in three-components is free of the 180 degree ambiguity of azimuth inherent in L_g particle motion (and in the observations of P in the horizontal plane alone, as above). The average error in estimated azimuth (from the true geodesic azimuth) over the entire data set is 7.0 degrees for the 3-component P processor (9.1 degrees rms). Setting an F threshold which rejects only 13 percent of the estimates reduces the average azimuth error to less than 6.0 degrees (7.4 degrees rms).

Since P waves may be emergent as well as impulsive (see Figures 8 and 9), the three-component P process was not simply applied to the one arrival window chosen by the analyst, but was allowed to search that vicinity with a sliding window. Of the several resulting estimates, those with unacceptably low emergence angles (less than 20 degrees from the horizontal) were rejected and the azimuth was picked from those remaining on the basis of the F-statistic.

Combining the estimated L_g azimuth with that of the P wave, simply by taking their mean, increased the accuracy. The average difference between the mean estimated azimuth and the true geodesic azimuth was 4.9 degrees (7.0 degrees rms). Moreover, the F-statistic computed by these processors serves to separate poor azimuthal estimates from the population: the azimuthal estimates (over 80% for this data set) which passed the arbitrary F threshold set for this study differed from the known geodesic azimuths by an average of 3.9 degrees (4.9 degrees rms). It is the author's experience that such accuracy is comparable to or better than that from a well-designed array of sensors.

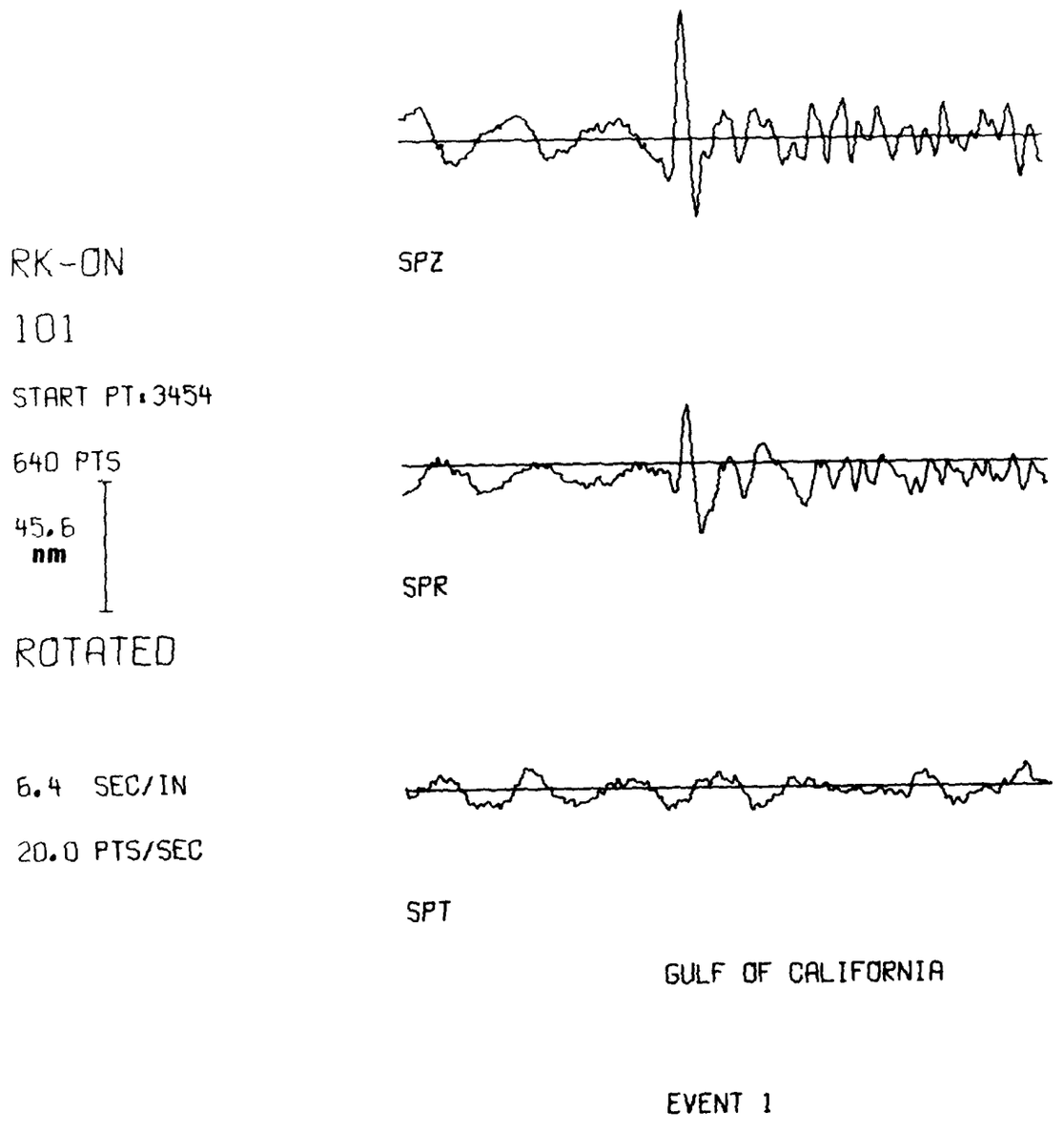

Figure 8. An impulsive P-wave signal selected from the present data set (see Table I, event 1).

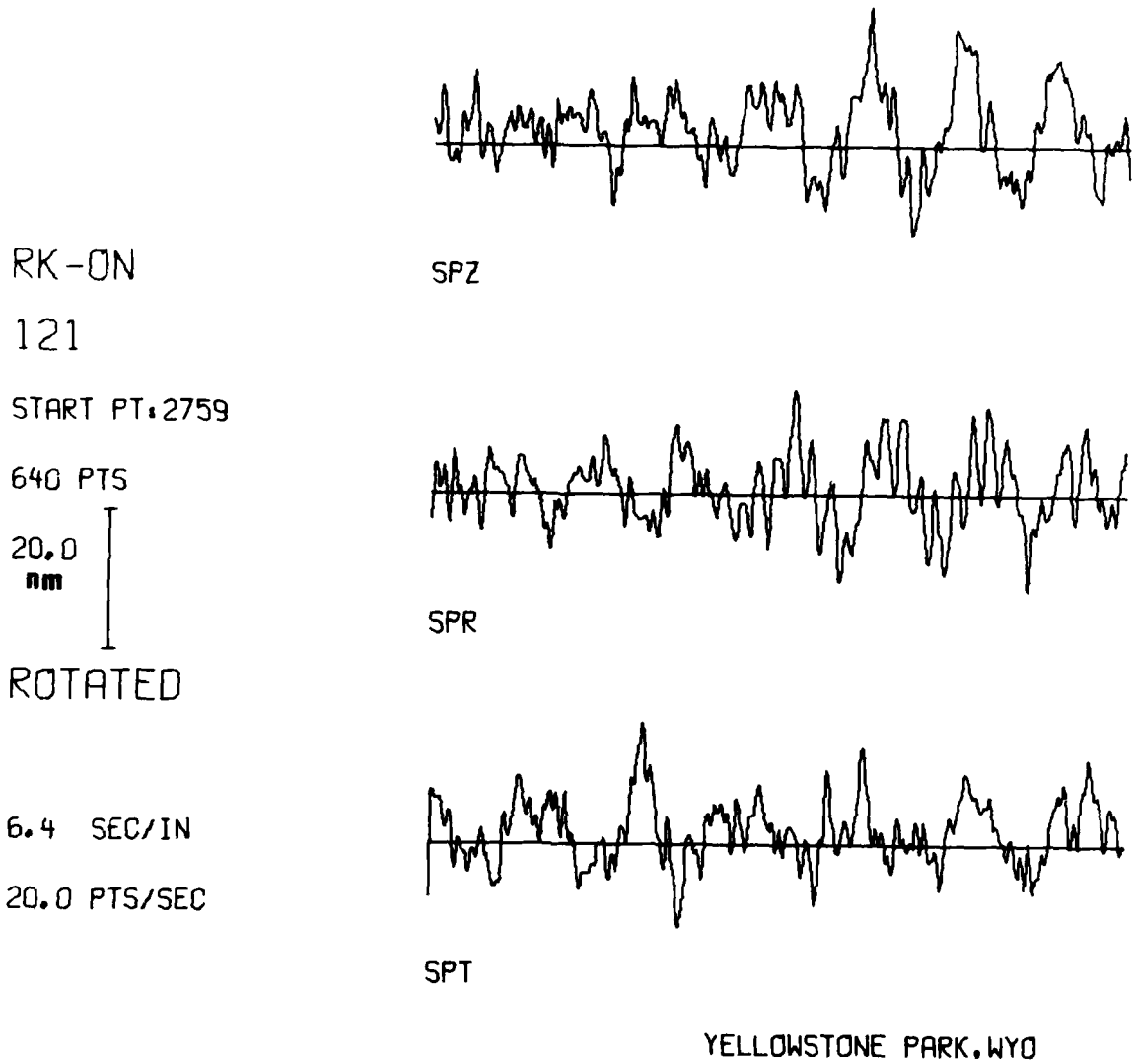

Figure 9. An emergent P-wave signal selected from the test data set of this study (see Table I, event 17).

Discussion

The limitations of this study have not permitted the conclusion of the research. The optimum frequency band, the optimum signal flag, and the most useful combination of P and L_g information have not been determined. Two additional detection criteria have suggested themselves during this work. One is the observed stability of orientation, over several time windows, of the elongated particle-motion envelope, both in the P-wave portion of the record and in the L_g portion. The other is the observed ninety degree rotation of the estimated azimuth as the P-wave passes and the L_g wavetrain arrives. These points demand further study.

The parameters estimated by the processors have not been fully exploited as yet. The emergency angle for P waves has been used here, and to good advantage, to avoid confusing L_g waves with P waves. They both have back-and-forth straight-line motion, but P motion is well out of the horizontal plane, while L_g motion is largely confined to it. Thus, the estimated emergency angle is an important criterion for P processing. But the ellipticity measurements from the surface-wave processor have yet to be employed. In this study, of RKON data, ellipticity clusters around 0.6, and the outliers are associated with inaccurate azimuths. Now that it is known to lie around 0.6 for RKON, the ellipticity can be held fixed, which will improve detection sensitivity, and may also bring those outliers in closer.

There are grounds for suspecting that the long time windows employed for L_g processing may have had an adverse effect upon the results of this study, at least as far as detection is concerned. Moreover, the three-component P processor has not been applied to noise to evaluate its sensitivity as a detector. So, further trials using various window lengths are in order.

Finally, it appears from the research carried out thus far, that the principal utility of particle-motion processing lies not in signal detection, where the simple power detector is successful, but in azimuth and distance determination. Of the missed signals in the P-wave detection trials discussed earlier, the P-wave processor estimated the back azimuth of half of them to within five degrees of their true back azimuth, even though it did not "detect" them. One of these signals was not visible even

to the analyst. The time between P and L_g, measured from the power rise at the signal onset down to the point where the particle-motion orientation rotates 90 degrees, yields a distance estimate. In the case of P-waves from sources at distances greater than 20 degrees from the recording station, the emergency angle also provides an estimate of source distance. Particle-motion processing can also be exploited for picking phases. All of this potential must be addressed in future research.

REFERENCES

Smart, E. (1977). A 3-component single-station maximum-likelihood processor, SDAC-TR-77-14, Teledyne Geotech, Alexandria, Virginia.

Archambeau, C. B., Bradford, J. C., Broome, P. W., Deen, W. C., Flinn, E. A. and R. L. Szx, 1965, Data processing techniques for the detection and interpretation of teleseismic signals, Proc. of the IEEE, 53, 1860-1884.